New Scaling Law for the Decay Exponent of Bimolecular Reactions in Unbounded Transitional Flows

P. Rogberg* and V. Cvetkovic
Royal Institute of Technology, 100 44 Stockholm, Sweden
(Received 22 July 2002; published 17 January 2003)

We propose a new scaling law for global kinetics of the stoichiometric reaction $A + B \rightarrow P$ in unsteady, transitional flows. We find in the nonlinear flow regime the decay as $\sim t^{-\alpha}$ where α is related to a space-time scaling parameter ψ as $\alpha \propto \psi^m$, for the considered parameter range $m = 0.067$. In the linear flow regime, we find that the maximum is $\alpha \simeq 2/3$ for $\psi \simeq 1$. The proposed scaling law should be useful for linking dynamical subgrid processes with reaction kinetics in a variety of transitional flow systems.

DOI: 10.1103/PhysRevLett.90.028303 PACS numbers: 82.20.–w, 05.40.–a, 47.20.–k, 47.70.–n

The dynamical impact of a flow field on bimolecular kinetics is of considerable interest in applied science such as combustion technology [1] and atmospheric chemistry [2,3], as well as from a more fundamental perspective [4–6]. The classical solution of $A + B \rightarrow P$, where A and B are two species and P is an inert product, is

$$\frac{d[A]}{dt} = -k[A][B], \tag{1}$$

where k is the reaction rate and $[\cdot]$ is the concentration defined over an elementary support volume, or area. Equation (1) is based on the assumption that the mixture is *well stirred* within the support volume, throughout the reaction process; this assumption leads to a decay of the type $[A] \propto t^{-\alpha}$ with $\alpha = 1$ for large t.

It is well established that bimolecular reactions such as (1) spontaneously generate clusters of A (respectively, B) in pure diffusive systems [7]. Since reactions take place only at the border of each cluster, these concentration fluctuations lead to a lower global decay rate compared to the classical $\alpha = 1/2$ decay [7].

In a more general situation where A and B are subject to additional advection (e.g., in a hydrodynamical context), the issue is less clear. Flows such as dilational flows [8], statistical mixing by tossing [9], or fully developed three-dimensional turbulence, act as efficient mixers and any cluster is rapidly destroyed by mixing leading to restoration of the classical $\alpha = 1$ decay.

There are important classes of flows, however, where the mixing is less efficient and varies in space. For instance, inviscid two-dimensional (2D) flows are generally slow mixers on a global scale, but locally develop spots with intense mixing [10], resulting in reaction kinetics which varies over the domain. Such flows are characterized by the existence of one or more long living coherent vortex structures separated from the embedding flow field by sharp vorticity gradients. The evolution of such vortices is due to the interaction with the surrounding field and typically leads to an unsteadiness of the vortex: the state of the vortex shifts between a dynamical phase where the vortex undergoes strong deformation leading to ejection of vortex filaments and a quasisteady state with small deformation [11]. Ocean eddies and the stratospheric polar vortex are examples of flows displaying such characteristics.

Previous studies have focused on bimolecular kinetics in a diffusive field [12], steady and homogeneous isotropic turbulence [4], steady shear flows [5], and von Karman vortex street [6]. Pure mixing properties in nonclassical flows have also been examined [13]. There are important issues related to the effect of *combined* dynamics and kinetics, however, which have yet to be resolved. One such issue is the scaling of global kinetic rates under transitional flow regimes.

In this Letter, we propose a new spatial and temporal scaling law for highly structured flows that undergo transition from a deterministic configuration to a chaotic state. We quantify for the first time global decay rates on the system scale, as functions of combined kinetic and dynamic mixing on a local scale, for unsteady, transitional flows. A new relationship for the decay rate exponent is established as a function of a single scaling parameter.

As a prototype for transitional flows, we consider a compressible, quasigeostrophic vortex column placed in a 2D laterally unbounded domain. The vortex is compressible in the sense that the density varies with height, $\rho_{\text{air}}(z) \propto \exp(-z)$, and it is vertically restricted by the no-flow condition at the top and bottom. Furthermore, there is an external forcing in the form of a background mean velocity field $\mathbf{U}$ and a variable vortex anomaly beneath the column. The forcing induces a perturbation which amplifies as it propagates up through the vortex due to decreasing density.

The flow evolution is related to the vorticity distribution by $q = \nabla^2\psi$, where ψ is the stream function and q is the vorticity [14]. Conventional grid-based or spectral techniques are not well suited for high-resolution studies of this flow class due to their inability to maintain sharp gradients [15]. We instead rely on a Lagrangian modeling

technique which integrates the vortex contours directly. The method, referred to as contour dynamics (CD), can be formulated for any 2D flow field which possesses a generalized vorticity invariant q. CD has been previously used for examining fundamental properties of general 2D flows [11,13] as well as in a geophysical context [15]. We emphasize that a high-resolution model is a requirement for accurately tracking the history of tracer particles and resolving small-scale reactions.

The particular form of q depends on the flow configuration; for a vortex column with topographic forcing, it is $q = \nabla^2\psi + \frac{1}{\rho}\frac{\partial}{\partial z}(\Lambda(z)\frac{\partial\psi}{\partial z}) - f_0\eta(\mathbf{x})$, where ρ is the density, $\Lambda(z)$ and f_0 are flow specific parameters, and η quantifies horizontal geometry and amplitude of the underlying forcing. The no-flow condition in the vertical direction gives $\frac{D}{Dt}(\Lambda\frac{\partial\psi}{\partial z}) = 0$ at $z = H$ and $\frac{D}{Dt}(\Lambda\frac{\partial\psi}{\partial z} - f_0\eta(\mathbf{x})) = 0$ at $z = 0$. The lower boundary condition is equivalent to choosing the surface $z = \eta(\mathbf{x})$ to be an isentrope, thus, by specifying η we can perturb the vortex column. The velocity field generated by the vortex is now obtained by integrating the vorticity within the vortex column as [16]

$$\mathbf{u}(\mathbf{x}) = -\int_0^H dz'\rho(z')q(z')\oint_\Gamma G(\mathbf{x}';\mathbf{x})d\mathbf{x}', \qquad (2)$$

where q is the vorticity jump across the vortex boundary Γ, $\mathbf{x}$ is a material coordinate, $G = -K_0(\gamma|\mathbf{x}-\mathbf{x}'|)/2\pi$ is the Green function for a quasigeostrophic fluid, K_0 is the modified Bessel function, and γ is a parameter. The model is extended with a *surgery* process [15] which involves removal of filamentary vorticity structures below a given cutoff scale δ. We consider the vortex when $-f_0\eta(\mathbf{x}) = 1.2q$ with $q = 2.0$ and $\mathbf{U} = (0.12, 0)$. Even though the forcing is stationary, it generates an unsteadiness and a nonreversible deformation which qualitatively mimics the dynamics of a winter time stratospheric polar vortex [16]. Suitable normalization parameters (that are used throughout) are related to the undisturbed vortex: one rotational period T for time and radius L for space.

At $t = 0$, dynamically inert particles A and B are distributed over an isentropic surface at the top of the vortex, following a uniform distribution. The location of each particle is given by $\mathbf{X}(t) = \int_0^t \mathbf{u}[\mathbf{x}(t')]dt' + \mathbf{U}t + \boldsymbol{\xi}$, where $\boldsymbol{\xi} = (2D\Delta t)^{1/2}\mathbf{e}$, D is a normalized diffusion coefficient, and $\mathbf{e}$ is a random vector with two components drawn from a normal distribution with zero mean and unit variance. The random displacement $\boldsymbol{\xi}$ quantifies the effects of motions at subgrid scales, consistent with a diffusion process, hence $\boldsymbol{\xi}$ is of zero mean and isotropic variance $2D\Delta t$. A snapshot of the vortex and particle distribution at $t = 10$ is illustrated in Fig. 1.

Let the bimolecular reaction be dependent on two parameters, ρ and τ, where $\rho \equiv |\mathbf{x}_A - \mathbf{x}_B|$ is the distance between two particles A and B, and τ is a temporal parameter. There are two effects we wish to emulate: the impact of spatial resolution on the global reaction rate and the impact of chemistry as quantified by the

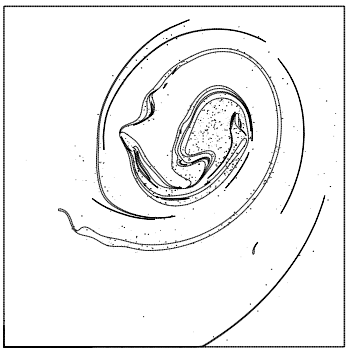

FIG. 1. The top layer of the vortex with particles seen from above at $t = 10$. Initially, the vortex is circular with a radius L ($L = 1/6$ of the box width). Nonlinear wave breaking, induced by the forcing, creates filamentary structures which become rapidly thinner and are ultimately removed from the vortex body. Because of random fluctuations, some particles have crossed the contour and moved with the external flow field.

local kinetic rate $1/\tau_c$. Let the probability of A and B particles reacting in the flow field be defined by

$$\text{Prob}\{A + B \rightarrow P\} = \begin{cases} 1 & \text{if } \rho \le \rho_c \wedge \tau \ge \tau_c, \\ 0 & \text{otherwise,} \end{cases} \qquad (3)$$

where ρ_c and τ_c are specified. We can view ρ_c as a critical radius of an unit area $\mathcal{A}(\rho_c)^i = \pi\rho_c^2$ ($i = A, B$) with a particle positioned at the center. When $\rho = \rho_c$, two areas overlap as $\mathcal{A}^{AB} \equiv \mathcal{A}^A \cap \mathcal{A}^B$, where $\mathcal{A}^{AB}$ can be interpreted as a support area for the chemical reaction given in material coordinates. The time τ_c characterizes local (intrinsic) reaction kinetics where the rate is $\sim 1/\tau_c$. The rule (3) is a material equivalent of what is commonly used in lattice systems, where particles, say A, jump from one lattice site to another, and a reaction depends on whether the new location is occupied by a B particle or not [17].

For $\tau_c = \Delta t$ (which equals one numerical time step), the discrete reaction (3) proceeds as follows. A neighborhood of radius ρ_c is defined for every particle A and B. If one particle of opposite type is found within, both particles will react and become P. If there is more than one particle of opposite type within a radius ρ_c, only the nearest particle participates in the reaction.

For $\tau_c = n\Delta t$ (where $n > 1$ is an integer), the area around a particle is scanned for possible reactants; particles which are found will be tracked during the next time step. If no opposite particle is found in the area, no reaction will occur. This process continues until $\tau = \tau_c$ when the particles react. If a particle pair initially is sufficiently close, but diverge such that $\rho > \rho_c$ during the time span $\Delta t < \tau < \tau_c$, the encounter process will terminate and the particle pair will continue as A (respectively, B).

In Fig. 2 we exemplify a typical decay process for different values of ρ_c with a relatively rapid reaction ($\tau_c = 0.025$). The curves of Fig. 2 are qualitatively

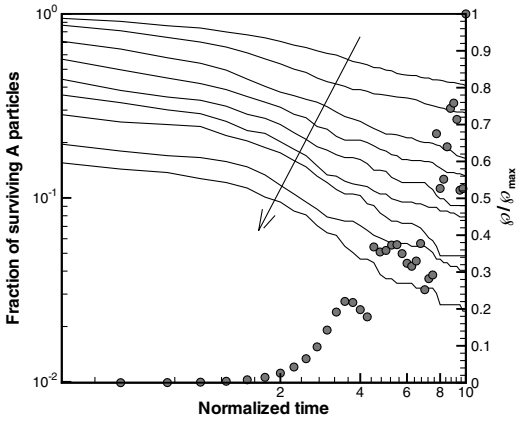

FIG. 2. Fraction of particles A remaining in the system, and departure from circularity $\wp$, as functions of time, for $\tau_c = 0.025$. The arrow is directed toward increasing ρ_c in the range 0.005–0.1. The initial drop for $t = \tau_c$ strongly depends on the initial particle distribution. The relatively slow decay of A particles characterizes the linear flow regime with $\wp \approx 0$. A strong increase of $\wp$ is indicative of the nonlinear flow regime, resulting in more rapid decay. Position of the breakpoint between regimes is around $t = 1$ and depends on ρ_c and τ_c. The curves are plotted from $t = 0.3$ which is the maximum τ_c considered.

consistent with results from previous studies of bimolecular kinetics in simpler flows systems, which have revealed the existence of multiple regimes for the decay rate [4]. These regimes are typically characterized by a power-law dependence where the decay rate depends on which process is dominant.

To highlight the link between global decay rate and flow dynamics, we also plot in Fig. 2 a time-dependent measure $\wp$ defined as $\wp \equiv 1/4 \oint_\Gamma r^4 d\theta - \mathcal{A}^2/2\pi$ [13,18]. This measure quantifies the deformation of the vortex induced by the flow dynamics, as the normal mean-square displacement of the vortex boundary Γ from a circular shape with area $\mathcal{A}$. The value $\wp \geq 0$ is based on a linear combination of vorticity and angular momentum (which are conserved for this flow), whereas $\wp = 0$ is applicable for a circular patch of vorticity [18]. Evolution of $\wp$ clearly distinguishes two regimes for global decay: linear flow with $\wp \approx 0$ up to $t \approx 1$ and relatively slow decay, and nonlinear flow regime in the range $1 \lesssim t < 10$ with a steep rise in $\wp$ and more rapid decay (Fig. 2).

Let $\mathrm{Pe} \equiv 4\pi^2 L^2/DT$ denote the global Peclét number, where $2\pi L/T$ is the characteristic (rotational) velocity and $2\pi L$ is the associated length; so defined, Pe provides a convenient measure of diffusive displacement relative to advective displacement. In order to study the impact of linear and nonlinear flow regimes on global kinetics, we introduce a dimensionless number ψ by combining the reaction parameters ρ_c and τ_c with Pe as

$$\psi \equiv \frac{\rho_c^2 \mathrm{Pe}}{\tau_c} \equiv \frac{4\pi^2 \rho_c^2}{\tau_c D}. \tag{4}$$

The decay is examined as a function of ψ in the linear (for $t \lesssim 1$) and nonlinear flow regime ($1 \lesssim t \leq 10$). The decay properties are examined for the parameter ranges of $0.005 \leq \rho_c \leq 0.1$, $0.025 \leq \tau_c \leq 0.3$, and $20 \leq \mathrm{Pe} \leq 8900$.

Consider the limits of ψ and α. A small value of ψ implies that ρ_c is small and therefore the probability that a reaction will occur is small [this follows from (3)]; consequently, the decay exponent α is small and $\alpha \to 0$ as $\psi \to 0$. The probability that the interparticle distance satisfies $\rho < \rho_c$ during $\tau \geq \tau_c$, initiating a reaction, decreases with a diminishing ρ_c. At the other end of the parameter range, where $\rho_c^2 \mathrm{Pe} \gg \tau_c$, the impact of dynamics decreases as the effect of fluctuations on scales below ρ_c diminishes.

The decay exponent is naturally bounded as $0 \leq \alpha \leq 1$, with $\alpha = 0$ applicable when no reaction takes place and $\alpha = 1$ applicable when particles are confined in a *perfect mixer,* reacting as soon as $\tau = \tau_c$. There is a distinct breaking point during the linear regime, $t \lesssim 1$, where α reaches a maximum for $\psi \approx 1$, hence we have maximal decay rate when $\tau_c/\rho_c^2 \simeq \mathrm{Pe}$ [Fig. 3(a)]. It is also apparent that the system is an imperfect mixer with $\alpha_{\max} \simeq 2/3$ [Fig. 3(a)]. The nonlinear regime is clearly different [Fig. 3(b)], with α positively correlated to ψ as

$$\alpha = \begin{cases} 0 & \psi < \psi_l \\ \psi^m & \psi_l < \psi < \psi_u \\ 1 & \psi > \psi_u \end{cases}, \tag{5}$$

where for the considered parameter range we have $m = 0.067$.

The piecewise formulation of Eq. (5) follows from the definition of the dimensionless number, ψ. The lower limit ψ_l mimics conditions when effectively no reaction takes place, because the reaction distance ρ_c is too small and/or reaction time is too large τ_c, hence $\alpha \to 0$. The upper limit of (5) also follows from (3): A large value of ρ_c implies that two particles can react at a relatively large distance. In the limit, when ρ_c equals the domain size, the system mimics a batch reactor, thus for ψ larger than ψ_u we have convergence to the classical case, $\alpha \to 1$, i.e., decay as t^{-1}. An increasing ψ essentially leads to a complete recovery of the classical $\alpha = 1$ decay in the nonlinear regime [Fig. 3(b)].

For comparative purposes, the bimolecular reaction (3) was considered in the same domain with particles A and B subject only to random fluctuations (diffusion), i.e., $\mathbf{X} = \boldsymbol{\xi}$. In such a case, we found an analogous pattern for ψ and α as that seen in Fig. 3(a), i.e., a distinct breakpoint and no apparent correlation between α and ψ [19]. For (5) to be applicable, therefore, the system has to maintain sufficient mixing.

Chaotic behavior of a vortex structure can be initiated in a variety of ways, for instance, with forcing functions that are either time dependent or have spatial variation. A forcing that produces efficient mixing must lead to

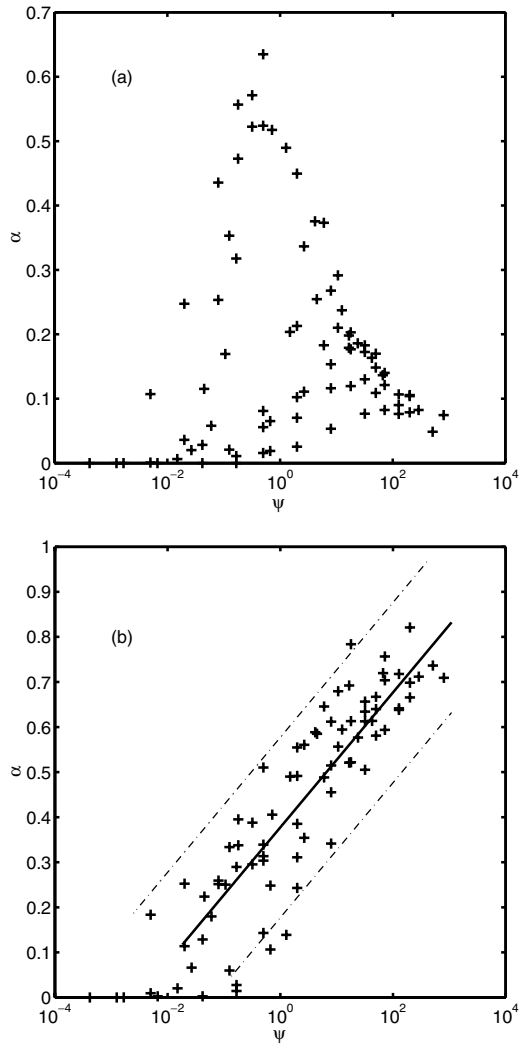

FIG. 3. The rate exponent α as a function of $\ln(\psi)$ for (a) linear flow regime and (b) nonlinear flow regime. A least-squares fit with 95% confidence interval is plotted in (b), $\alpha \propto \psi^{0.067\pm0.007}$, where 0.007 is the standard deviation of m; the correlation coefficient in (b) is 0.9.

increasing m. In the limit, an ideal mixer which instantaneously tosses A and B reactants around leads to a large m, while a forcing that generates no mixing is consistent with a linear flow regime. In our calculations, we chose as simple as possible forcing which maintains key features of nonlinear and transitional flows, such as increasing unsteadiness over time, and a continuous filamentation.

In conclusion, we have identified ψ (4) as the single controlling parameter for the decaying exponent α in the nonlinear flow regime. It combines spatial and temporal scales naturally arising in problems involving both kinetics and dynamics. The scaling law was shown to be robust with respect to random fluctuations for the considered parameter range. For the linear flow regime, we found that the decay rate has a maximum of $\alpha \simeq 2/3$ for $\psi \simeq 1$. The unique character of the semianalytical CD simulation tool is in that it can resolve scales even for realistic unsteady flow systems, such as the polar vortex. Previous studies of bimolecular reactions have been either in lattice structures [12,17] or in simpler flows regimes [1,4–6]. Current results verify (5) for a 2D quasigeostrophic flow only. However, given the features of this flow which are characteristic of transitional flows in general, and the unprecedented particle tracking accuracy of the CD algorithm, we hypothesize (5) to be applicable for a wider class of transitional flows with coherent structures.

Typical applications with grid-based models (such as global circulation models) introduce their own scales due to restricted resolution. A resulting effect is that in most cases small-scale dynamics are unresolved and subgrid structures act as perfect mixers; this in turn can lead to incorrect parametrization of reaction kinetics [3,20]. The parameter ψ in (4) relates the spatial resolution ρ_c, temporal scales of chemical reactions (τ_c), and subgrid mixing processes quantified by Pe, arising, for instance, in grid-based models. The scaling law (5) presented in this Letter can then become a useful tool for evaluating the parametrization of kinetic reactions, in a wide range of unsteady and transitional flows.

*Electronic address: rogberg@kth.se

[1] R. G. Rehm *et al.*, Combust. Sci. Technol. **91**, 143 (1993).
[2] D. G. H. Tan *et al.*, J. Geophys. Res. **103**, 1585 (1998).
[3] S. Edouard *et al.*, Nature (London) **384**, 444 (1996).
[4] R. Reigada *et al.*, J. Chem. Phys. **105**, 10 925 (1996).
[5] M. J. Howard and G. T. Barkema, Phys. Rev. E **53**, 5949 (1996).
[6] Z. Torocazki *et al.*, Phys. Rev. Lett. **80**, 500 (1998).
[7] D. Toussaint and F. Wilczek, J. Chem. Phys. **78**, 2642 (1983).
[8] I. M. Sokolov and A. Blumen, Phys. Rev. Lett. **66**, 1942 (1991).
[9] P. Argyrakis and R. Kopelman, J. Phys. Chem. **93**, 225 (1989).
[10] D. Elhmaïdi, A. Provenzale, and A. Babiano, J. Fluid Mech. **257**, 533 (1993).
[11] D. G. Dritschel, J. Fluid Mech. **293**, 269 (1995).
[12] K. Kang and S. Redner, Phys. Rev. Lett. **52**, 955 (1984).
[13] P. Rogberg and D. G. Dritschel, Phys. Fluids **12**, 3285 (2000).
[14] B. J. Hoskins, M. E. McIntyre, and A. W. Robertson, Q. J. R. Meteorol. Soc. **111**, 877 (1985).
[15] D. G. Dritschel, Comput. Phys. Rep. **10**, 77 (1989).
[16] D. G. Dritschel and R. Saravanan, Q. J. R. Meteorol. Soc. **120**, 1267 (1994).
[17] F. Leyvraz and S. Redner, Phys. Rev. Lett. **66**, 2168 (1991).
[18] D. G. Dritschel, J. Fluid Mech. **191**, 575 (1988).
[19] P. Rogberg and V. Cvetkovic (to be published).
[20] J. Thuburn and D. G. H. Tan, J. Geophys. Res. **102**, 13 037 (1997).